Z. Phys. B - Condensed Matter 57, 329–333 (1984)

Condensed Matter
Zeitschrift für Physik B

Transient Patterns of the Convection Instability: A Model-Calculation

M. Bestehorn and H. Haken
Institut für Theoretische Physik 1, Universität Stuttgart, Federal Republic of Germany

Received August 8, 1984

Using a recently derived non-linear partial differential equation describing the temperature field we have performed computer calculations on the evolving convection patterns in different geometries. In this way we calculate the generation of various patterns e.g. of rolls or hexagons.

1. Introduction

The formation of convection patterns in fluid layers heated from below has been subject to numerous experimental and theoretical studies (for a list of references see e.g. [1, 2, 3]).
The basic work by Schlüter et al. [4] and Segel [5] was carried further, in particular by Newell and Whitehead [6]. The latter authors derived equations for the mode amplitudes including their slow temporal change and finite band width excitations.
Graham [7, 8] and Haken [9, 10] extended the treatment to include fluctuating forces. The latter included effects which violate the inversion symmetry of the central horizontal layer in the liquid. It had been shown previously (e.g. [11]) that these effects can give rise to hexagons while without them only rolls are formed.
An elegant equation for the formation of rolls was derived by Swift and Hohenberg [12]. Their equation was solved numerically under rectangular geometries [13] and shows the build-up of rolls. A detailed analytical study based on Lyapunov-functions has been performed by Cross [14]. The present paper is based on generalized Ginzburg Landau equations [3] which describe in particular the convection instability and which were condensed into a convenient equation for a field amplitude $\Psi(\mathbf{x}, t)$.

2. The Basic Equation

Starting from the Navier Stokes equations, the heat equation and the continuity equation, one can derive an order parameter equation in the form of a partial differential equation for a two-dimensional time dependent function Ψ which is proportional to the horizontal disturbances of the steady temperature field [15]. In lowest nontrivial order this equation reads:

$$\dot{\Psi}(\mathbf{x}, t)=[\varepsilon-(1-\Delta)^2]\Psi(\mathbf{x}, t)+\delta\Psi^2(\mathbf{x}, t)-\Psi^3(\mathbf{x}, t) \tag{1}$$

where $\delta=0$ if the Boussinesq-approximation is valid. This equation had been derived for the special case $\delta=0$ by Swift and Hohenberg in an entirely different fashion [12]. The individual terms of that equation were discussed by Cross [16]. The simplest way to include non-Boussinesq-terms in the Navier Stokes equations is to extend the temperature dependence of the density:

$$\rho(T)=\rho_0[1-\gamma(T-T_0)+\tilde{\gamma}(T-T_0)^2] \tag{2}$$

where $\tilde{\gamma}$ vanishes in the Boussinesq-approximation (e.g. [2]). Other possibilities are given by the temperature dependence of the viscosity [17] or of the thermometric conductivity, or by the influence of the surface tension on a stress - free upper surface by introducing another parameter, called Marangoni-number [18, 1].

3. The Meaning of Ψ, Boundary Conditions

Let $\mathbf{v}$ be the three-dimensional velocity field and θ the deviations from the steady temperature field. In

the lowest order of Ψ we obtain the relations:

$$v_i = \frac{\partial f(z)}{\partial z}\frac{\partial \Psi(\mathbf{x},t)}{\partial x_i} \quad i=1,2$$
$$v_3 = f(z)\Delta\Psi(\mathbf{x},t) \tag{3}$$
$$\theta = g(z)\Psi(\mathbf{x},t),$$

where the functions $f(z)$ and $g(z)$ are fixed by the linear problem and by the boundary conditions in the z-direction [19]. If we assume free boundary conditions in the x_1-x_2 - plane and vanishing θ on the boundaries, equations (3) lead to:

$$\Psi(\mathbf{x}) = \frac{\partial \Psi(\mathbf{x})}{\partial \mathbf{n}} = 0 \tag{4}$$

for $\mathbf{x}$ on the sidewalls and $\mathbf{n}$ perpendicular to them.

4. Lyapunov-Functional

An important property of (1), not only for the numerical treatment, is the existence of a potential L, called Lyapunov-functional [14, 7, 10, 3] from which one can variationally derive (1), so that

$$\frac{\partial \Psi}{\partial t} = -\frac{\delta L[\Psi]}{\delta \Psi} \tag{5}$$

where $L[\Psi]$ is given by

$$L[\Psi] = \tfrac{1}{2}\int\int dx_1 \cdot dx_2 [-\varepsilon\Psi^2 - \tfrac{2}{3}\delta\Psi^3 + \tfrac{1}{2}\Psi^4 + ((\Delta+1)\Psi)^2]. \tag{6}$$

For metastable or stable states of the system, $\frac{\delta L[\Psi]}{\delta \Psi} = 0$. In the absence of any fluctuations, L can be shown to be a Lyapunov-functional in the strict sense, decreasing monotonically with time until a metastable or absolutely stable state is reached, which, however, requires an infinitely long time. Stability-analysis based on the Lyapunov-potential defines regions in the $\varepsilon-\delta$-plane where rolls, hexagons or even both patterns are stable (Fig. 1, see also [20]). In the latter case the resulting patterns will depend on the initial conditions.

5. Numerical Results

To solve the equation (1) on a computer (VAX 11/750), we apply a forward Euler time integration scheme leading to a nonlinear set of equations of the form

$$\Psi(\mathbf{x}, t_{n+1}) = \Psi(\mathbf{x}, t_n) + [L\Psi(\mathbf{x}, t_n) + \delta\Psi^2(\mathbf{x}, t_n) - \Psi^3(\mathbf{x}, t_n)]\,\Delta t_n \tag{7}$$

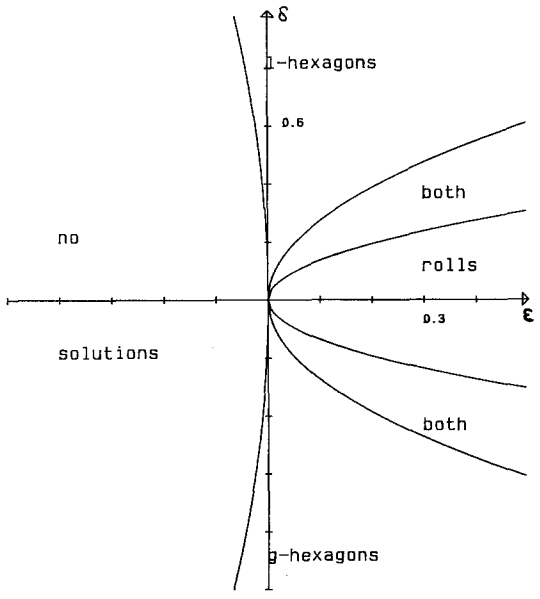

Fig. 1. Stability regions for hexagons and rolls in the $\varepsilon-\delta$-plane. There exists a region where both patterns are stable

where L is a linear biharmonic operator, and

$$t_{n+1} = t_n + \Delta t_n$$

$\Psi(\mathbf{x}, t_0)$ is the initial field, which represents random domains.

L is calculated for a mesh of k times l points by using a finite difference method. In our numerical experiments we used mesh sizes of 100×100 up to 160×160 points, depending on the geometry and the aspect ratio of the layer.

Starting from (6) one can easily calculate the Lyapunov-function. Under the boundary conditions (4), (6) reads:

$$L[\Psi] = -\tfrac{1}{2}\int dx_1 dx_2 \left(\frac{\Psi^4}{2} - \frac{\delta}{3}\Psi^3 + \Psi\dot{\Psi}\right). \tag{8}$$

The integral can be approximated by a double sum running over k and l. A typical time behaviour of L is shown in Fig. 2 for the transition from a random

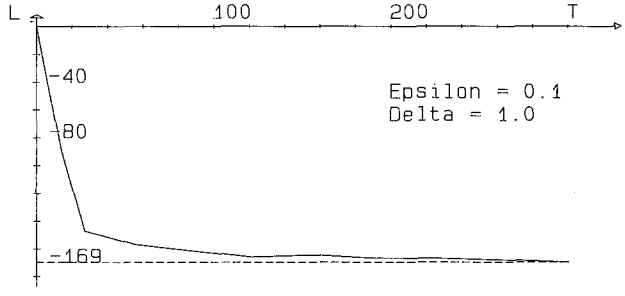

Fig. 2. Typical time dependence of a Lyapunov-function, here for the transition from a random dot pattern to a hexagonal pattern (see also Fig. 3)

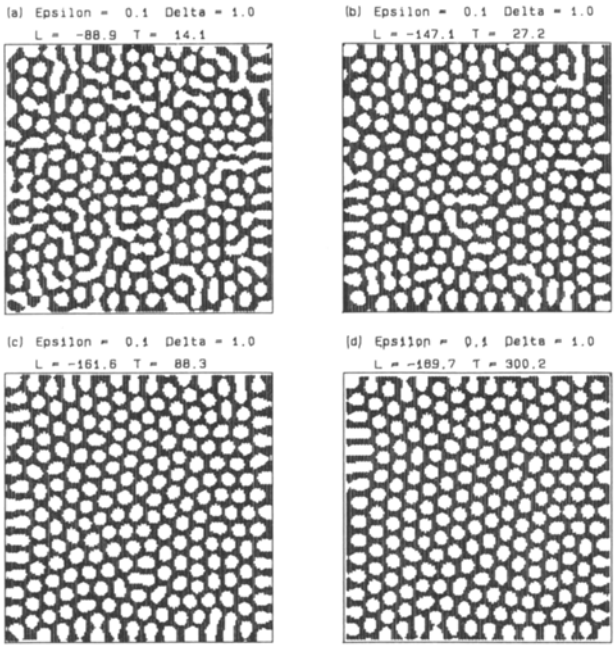

Fig. 3. Domains of positive (white) and negative (black) temperature-field Ψ at various times t. The initial condition was random-dot. L is the Lyapunov functional. The cells have an aspect ratio of 32, the parameters are in the hexagonal region

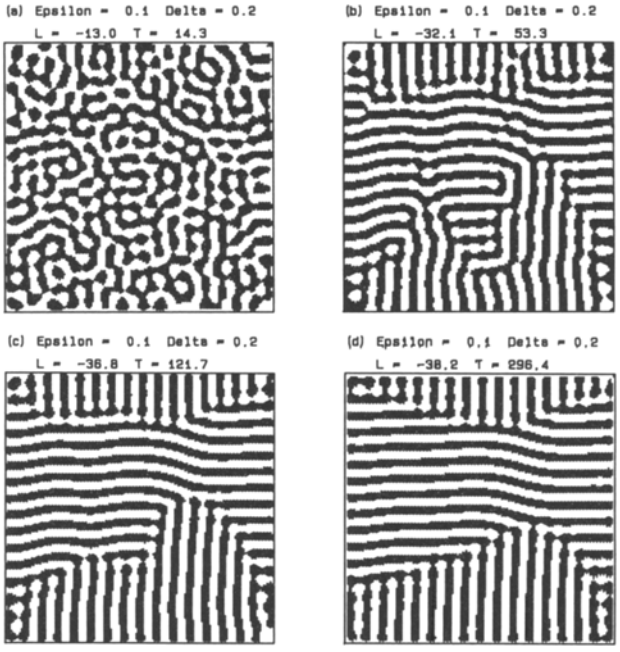

Fig. 5. Same as in Fig. 3, but for a pair of parameters in the metastable region

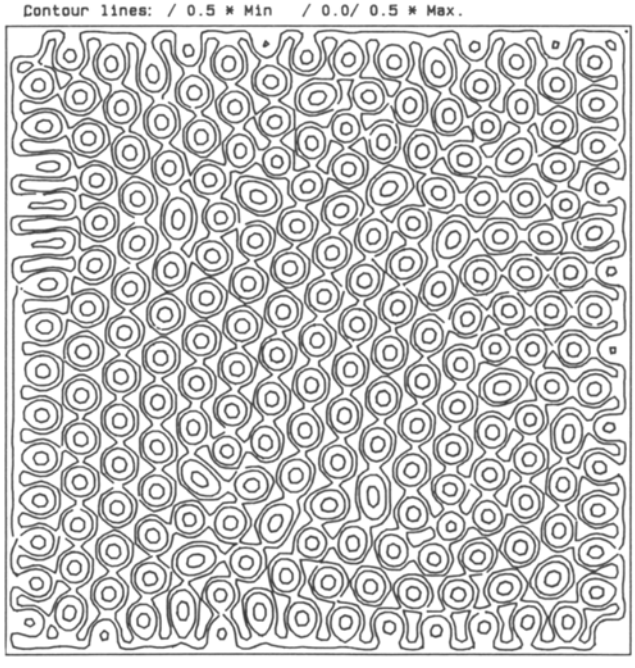

Fig. 4. Contour plot of the last state in Fig. 3

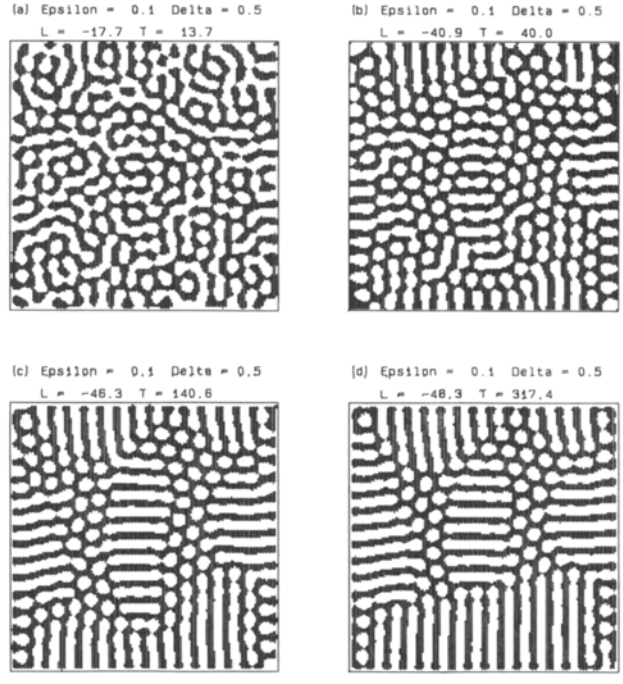

Fig. 6. Situation for $\varepsilon = 0.1$, $\delta = 0.5$, just in the hexagonal region

dot pattern as initial condition to hexagons (see below).

We examine the time development for random dot patterns as initial condition for different geometries of the layers and parameter values. Fig. 3 shows the development of a hexagonal pattern. Here and in the next two figures the aspect ratio is 32. The parameters are $\varepsilon = 0.1$, $\delta = 1.0$, the mesh consists of 160×160 points.

Another series is represented in Fig. 5. We used the same random dot state as in Fig. 3 but the parameters were now in the metastable region ($\varepsilon = 0.1$, $\delta = 0.2$) and a roll pattern resulted. Now we change the parameters again such that we are just in the

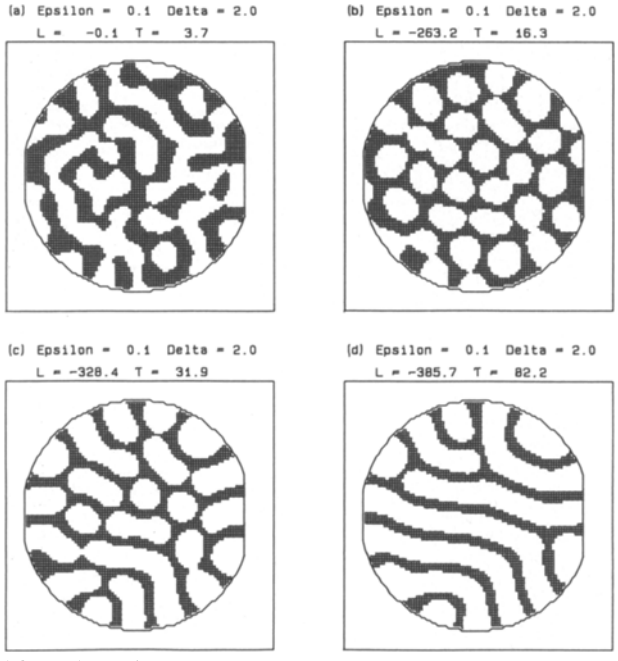

Fig. 7. A random dot pattern as initial condition for an almost cylindrical cell. The parameters are in the hexagonal region, but the hexagons formed after $T \simeq 16$ are not stable because of the influence of the side walls

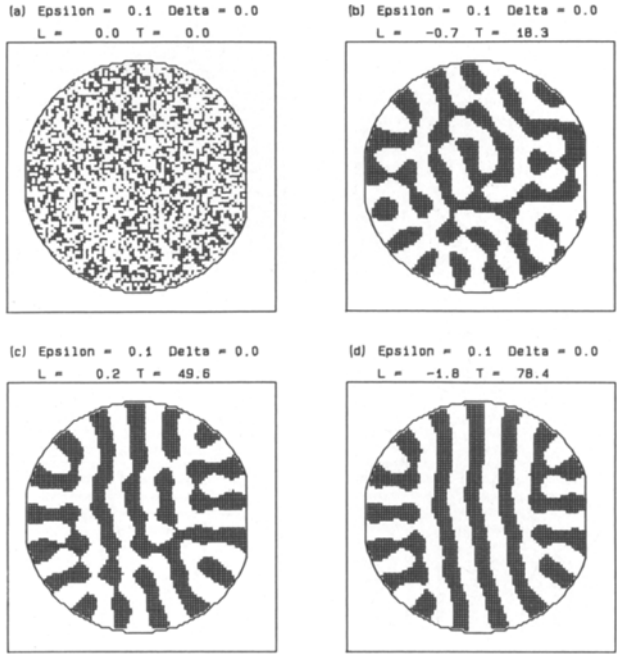

Fig. 8. Same as in Fig. 7, but for $\delta = 0$. One can see, only parallel rolls are formed

hexagon region ($\varepsilon = 0.1$, $\delta = 0.5$) and obtain Fig. 6. As one sees, even for these parameters rolls are formed in large parts of the layer, in the main near the sidewalls.

With our numerical method we are able to approximate arbitrary sidewalls of the layer. Figures 7 and 8 give another example where we used a geometry close to a circular. The parameters in Fig. 7 were in the hexagon region and hexagons were in fact formed in the first part of the transition but then the rolls grew from the sidewalls and a pattern resulted which we know from experiments in cylindrical cells* [21].

To examine the influence of the square term in our basic equation for this geometry we performed the same calculation with $\delta = 0$ and $\varepsilon = 0.1$. The quite different result is shown in Fig. 8. If we compare our results with the experiments performed by Bergé and Gollub, we see that non-Boussinesq effects obviously play there an important role.

All these pictures are in good qualitative agreement with experimental findings (e.g. Bergé and Dubois [23], Koschmieder [24], Gollub and Steinmann [25]). After a rather fast transition period the final state is approached only asymptotically. This effect called "critical slowing down" is well known from nonequilibrium phase transitions [3].

6. Fourier Spectra

In order to study which modes take part in our solutions, we make a Fourier transformation of the form

$$A(\mathbf{k}) = \int dx_1\, dx_2\, \Psi(\mathbf{x}) \exp[i\mathbf{k}\mathbf{x}]$$

which can be approximated by a double sum running over the mesh points.

Figure 9 shows the real part of $A(\mathbf{k})$ as a function of k_x and k_y for the pattern in Fig. 6d. As one sees, the excited modes describe a circle with the radius $|k_c|$. The four peaks on the axis correspond to the two main directions of the rolls perpendicular to the sidewalls in Fig. 6d.

The transformation of the hexagonal pattern (Fig. 3d) is shown in Fig. 10. To obtain more information, we sum up $|A(\mathbf{k})|^2$ over $|k|$ as a function of the angle ϕ in the $k_x - k_y$-plane. The result is shown in Fig. 11 where the three directions of $\mathbf{k}$ which form the hexagonal cells are evident.

The same technique, but for patterns obtained by the experiment was performed by Gollub and McCarriar [26], who examined the Fourier spectra of roll patterns for several Rayleigh-numbers.

* At the recent Nobel Symposium "The Physics of Chaos and related Phenomena" J. Gollub showed experimental results, which are in good qualitative agreement with Fig. 7, presented by one of us (*H.H.*) at the same Symposium

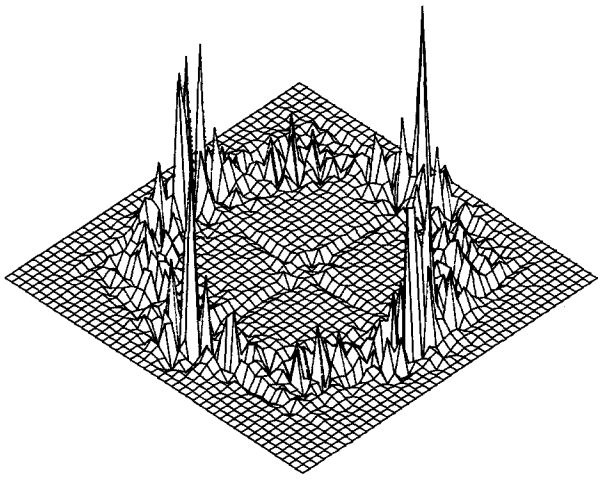

Fig. 9. Two dimensional Fourier-spectrum of Fig. 6d. Only modes with $|\mathbf{k}| \simeq |\mathbf{k}_c|$ take part in the final state

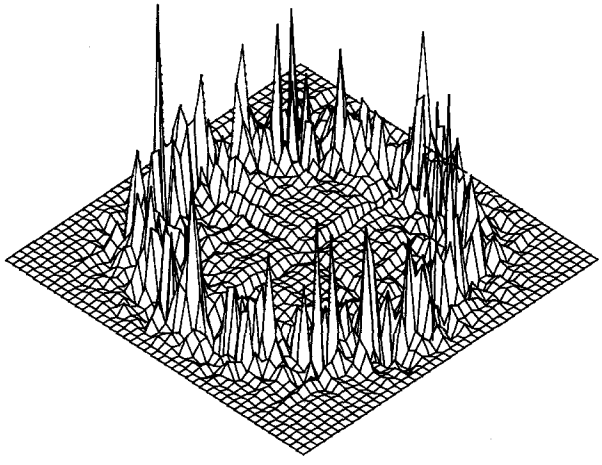

Fig. 10. Same as in Fig. 9, but for the hexagonal pattern in Fig. 3d

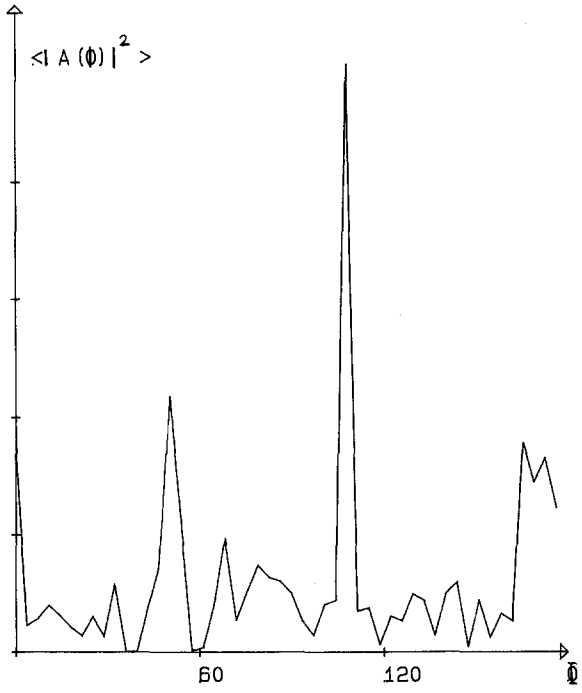

Fig. 11. Angular dependence of the mean value of $|A(\mathbf{k})|^2$ integrated over $|\mathbf{k}|$. The three peaks correspond to the three modes which build up the hexagonal solution

References

1. Normand, C., Pomeau, Y., Velarde, M.: Rev. Mod. Phys. **49**, 581 (1977)
2. Busse, F.: Rep. Prog. Phys. **41/II**, 1931 (1978)
3. Haken, H.: Synergetics. An Introduction. 3rd Edn. Berlin, Heidelberg, New York: Springer 1983
4. Schlüter, A., Lortz, D., Busse, F.: J. Fluid Mech. **23**, 129 (1965)
5. Segel, L.: J. Fluid Mech. **21**, 359 (1965)
6. Newell, A.C., Whitehead, J.A.: J. Fluid Mech. **38**, 279 (1969)
7. Graham, R.: Phys. Rev. Lett. **31**, 1479 (1973)
8. Graham, R.: Phys. Rev. **A 10**, 1762 (1974)
9. Haken, H.: Phys. Lett. **46 A**, 193 (1973)
10. Haken, H.: Rev. Mod. Phys. **47**, 67 (1975)
11. Busse, F.: J. Fluid Mech. **30**, 625 (1967)
12. Swift, J., Hohenberg, P.C.: Phys. Rev. **A 15**, 319 (1977)
13. Greenside, H.S., Coughran, W.M., Jr., Schryer, N.L.: Phys. Rev. Lett. **49**, 729 (1982)
14. Cross, M.: Phys. Rev. **A 25**, 1065 (1982)
15. Haken, H.: Advanced Synergetics. Berlin, Heidelberg, New York: Springer 1983
16. Cross, M.: Phys. Fluids **23**, 1727 (1980)
17. Palm, E.: J. Fluid Mech. **8**, 183 (1960)
18. Davis, S., Segel, L.: Phys. Fluids **11**, 470 (1968)
19. Chandrasekhar, S.: Hydrodynamics and hydromagnetic stability. Oxford: Oxford University Press 1961
20. Busse, F.: In: Pattern formation and pattern recognition. Haken, H. (ed.). Berlin, Heidelberg, New York: Springer 1979
21. Bergé, P.: In: Chaos and order in nature. Haken, H. (ed.). Berlin, Heidelberg New York: Springer 1981
22. Gollub, J.P.: Communication at the Nobel Symposium on "The Physics of Chaos and related Phenomena", Graftavallen, Sweden, June 1984
23. Bergé, P., Dubois, M.: Phys. Rev. Lett. **32**, 1041 (1974)
24. Koschmieder, E.L.: Adv. Chem. Phys. **26**, 177 (1974)
25. Gollub, J.P., Steinman, J.F.: Phys. Rev. Lett. **47**, 505 (1981)
26. Gollub, J.P., McCarriar, A.R.: Phys. Rev. **A 26**, 3470 (1982)

M. Bestehorn
H. Haken
Institut für Theoretische Physik I
Universität Stuttgart
Pfaffenwaldring 57
D-7000 Stuttgart-80
Federal Republic of Germany